Letters

Presynchronization of Weak Source in Microgrid

Tejaskumar Patel, *Student Member, IEEE*, and Priyesh Chauhan, *Member, IEEE*

***Abstract*—This letter deals with connection of a master-slave controlled microgrid with a grid or an alternative grid-forming source (AGFS). To match the microgrid frequency, phase and voltage with those of the incoming AGFS, a grid forming master VSC uses secondary control, typically in form of a pre-synchronization to make such connection seamless, whether the microgrid is grid-interactive or standalone. However, the contemporary control techniques are sluggish, cause phase-frequency interplay, transients, phase jumps, and notably, they do not deal with a weak incoming source. These limitations are addressed by a novel pre-synchronization control presented in this letter. The proposed technique is simulated using MATLAB/Simulink and validated on a lab test-bench by implementing the control algorithm on a DSP platform. The control performance shows a quick and transient-free pre-synchronization even under disturbances in the AGFS output.**

***Index Terms*—AC microgrid, master-slave control, presynchronization, seamless transition, secondary control.**

I. Introduction

AC MICROGRIDS in master-slave configuration typically have a battery energy storage (BES) operating as a master and the remaining distributed energy resource (DER), if any, as the slave(s). Fig. 1 shows such microgrid having two slave and a master DERs, each interfaced via their individual front-end voltage source converter (VSC). Each slave DER operates in grid-following (GF_o) mode using active–reactive power (P-Q) control. In presence of an alternative grid-forming source (AGFS), like utility grid or an alternator, the master operates in GF_o mode. When the AGFS is not available, the master operates in grid-forming (GF) mode using voltage–frequency (V-f) control [1]. During disconnection or reconnection of the AGFS, the mode of the master is switched from GF_o to GF and vice-versa. During the re/connection, the conditions for synchronization are met by matching the microgrid frequency, phase and voltage with those of the incoming AGFS [2]. The main challenge here is to achieve the synchronization swiftly and seamlessly without transients in the microgrid frequency and phase. For this purpose, a secondary control of the master DER sets various reference commands for the primary GF control. This is known as presynchronization technique [3], [4], [5], [6], [7], [8], [9], [10], [11], [12], [13], and its evolution is reviewed hereunder.

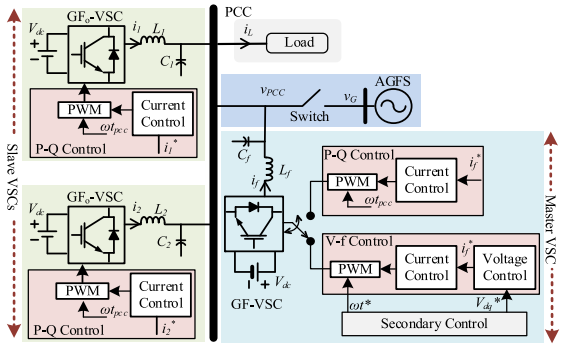

Fig. 1. Structure of AC microgrid with master-slave control.

Open-loop frequency (f)-variation technique: Some simpler methods changed the operating frequency of the GF-VSC for phase (θ) matching [3], [4]. But it cannot match f and θ at the same time; being an open-loop assisted process, it requires continuous monitoring of θ matching instant; and takes longer time when the frequency of the two sources are closer. While waiting for the θ matching instant, if the AGFS frequency gets disturbed, the matching duration becomes unpredictable and many a times much longer.

Closed-loop θ-error (θ_e) based f-variation technique: Here, a proportional—integral (PI) controller processes θ_e to modify the GF-VSC frequency in order to match both f and θ together [5], [6], [7]. But it introduces f transient upon enabling loop and subsequent f transients of varying magnitude depending on θ_e. The f-θ interplay extends their settling time. These problems worsen further, if the AGFS is a weak source.

Closed-loop $\sin\theta_e$ or $\cos\theta_e$-based f-variation technique: In improved versions of the aforesaid techniques, a PI controller processes $\mathrm{co/sin}\theta_e$ instead of θ_e [8], [9] to eliminate the f transients due to θ jumps, but it is unable to avoid the f transient upon enabling the loop and has longer settling time due to f-θ oscillations caused by the interplay between them.

Observations on f-variation techniques: The methods in [5], [6], [7], [8], and [9] attempt to match f and θ of two sources using single loop. Here, θ_e or $\mathrm{co/sin}\theta_e$ is processed to produce f

Manuscript received 4 December 2023; revised 15 January 2024 and 15 February 2024; accepted 4 March 2024. Date of publication 1 April 2024; date of current version 4 September 2024. *(Corresponding author: Priyesh Chauhan.)*

The authors are with the Department of Electrical and Computer Engineering at Institute of Infrastructure, Technology, Research and Management, Ahmedabad 380026, India (e-mail: tejas.patel.19pe@iitram.ac.in; priyeshchauhan@iitram.ac.in).

Color versions of one or more figures in this article are available at https://doi.org/10.1109/TPEL.2024.3383923.

Digital Object Identifier 10.1109/TPEL.2024.3383923

TABLE I
COMPARISON OF PRESYNCHRONIZATION SCHEMES

Comparison Criteria	*Technique A	Technique B	Technique C	Technique D	Technique E	Technique F	Technique G	Proposed Technique
f transient on enabling pre-sync	No feature of enabling	Present	Present	No feature of enabling	Present	No feature of enabling	Present	Absent
Repetitive f transients during pre-sync	Absent	Present	Absent	Absent	Present	Absent	Present	Absent
θ - f interplay	Present	Present	Present	Present	Present	Moderate	Moderate	Marginal
Interaction among f–θ–V loops	No control loops	Strong	Strong	No control loops	Strong	No control loops	Moderate	Marginal
Convergence time	Higher	Higher	Higher	Higher	Higher	Higher	Higher	Lower
Influence of disturbance in f of incoming source	Present, but not studied	Present, but not studied	Present, but not studied	Present, but not studied	Present, but not studied	Present, but not studied	Present, but not studied	Investigated, not noticeable
Use of measured signal from microgrid for feedback control	Used	Used	Used	Used	Used	Used	Used	Not used
θ jump on enabling pre-sync	No feature of enabling	Absent	Absent	Present	Present	Present	Present	Absent
Repetitive θ jumps during pre-sync	Absent	Absent	Absent	Absent	Present	Present	Present	Absent
Influence of jump in θ of incoming source	Present, but not studied	Present, but not studied	Present, but not studied	Present, but not studied	Present, but not studied	Present, but not studied	Present, but not studied	Investigated, not noticeable

* A: Open-loop f-variation, B: Closed-loop θe based f-variation, C: Closed-loop $co/sin\theta e$ based f-variation, D: Open-loop θ-variation, E: Closed-loop θ-variation, F: Open-loop f-θ-variation, G: Closed-loop f-θ-variation.

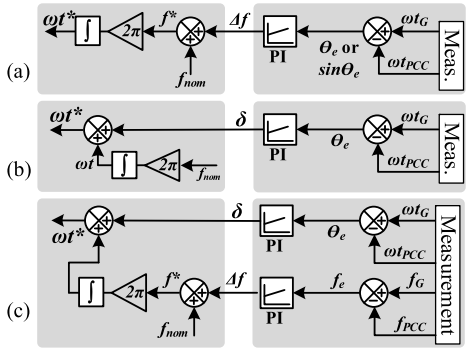

Fig. 2. Schematic representation of (a) f-variation techniques, (b) θ-variation techniques, and (c) f-θ-variation techniques for pre-synchronization.

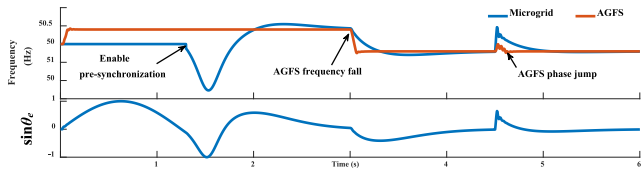

Fig. 3. Performance of (a) frequency matching and (b) phase ($\sin\theta_e$) matching with f-variation techniques.

deviation that can reduce θ_e. However, when the θ get matched, the f may be different, and that causes yet another θ deviation. As a result of this interplay between f and θ, an error in one quantity keeps causing deviation in the other until the both eventually converge together. Further, these methods assume that f and V of the AGFS remain constant during presynchronization. But if the AGFS is a weak source and its output gets disturbed during presynchronization, then f and θ diverge again, making the process even more sluggish.

Open- and closed-loop θ-variation techniques: The methods based on direct θ-variation facilitate θ matching, and avoid f transient [10], [11]. The open-loop technique [10] brings θ jump at the time of enabling the presynchronization, while the closed-loop technique [11] causes continuous θ jumps of varying magnitude depending on θ_e processed by the PI controller. Importantly, these methods do not consider f matching, without which, the θ matching is attained only momentarily due to f-θ interplay.

Open-loop f-θ-variation technique: A recent method uses direct θ-variation along with a separate f matching using f-variation [12]. This open-loop method avoids momentary θ matching, the f-θ interplay and f-transient by adjusting them one by one. However, a step change in f and θ compensation of the GF-VSC during f matching to avoid θ jump are undesirable. Also, the size of sampled θ_e and thereby the time of matching are affected by the instances of θ_e sampling and f matching. If f of AGFS changes during presynchronization, repeated attempts are required to attain the match.

Closed-loop f-θ-variation technique: A closed-loop version of the above technique employs separate f and θ controls [13]. The f control is enabled first, and the θ control is enabled after f matching. This eliminates f transients and avoids f-θ interplay. However, a θ jump appears upon enabling θ loop, and subsequent θ jumps occur due to θ_e jumps at input of PI controller. Enabling the loops one by one slows the process. Moreover, if f of AGFS gets disturbed during an ongoing θ matching process, the θ loop has to be disabled and the f matching has to restart. This adds delays.

The techniques reviewed above are shown schematically in Fig. 2, and compared in Table I. Some of the critical limitations of the f-variation techniques [5], [6], [7], [8], [9], and those of the θ- and f-θ-variation techniques [10], [11], [12], [13] are illustrated in Figs. 3 and 4, respectively.

The evolution of the presynchronization techniques presented above reflects the need for addressing various issues, such as f transients, θ jumps, convergence time, and f-θ interplay, which are not noticed in the earlier works. None of the existing methods considers disturbance in f-θ-V of the incoming AGFS during synchronization. All the methods also suffer from interaction

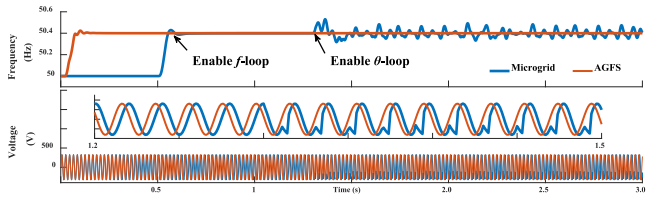

Fig. 4. Performance of (a) frequency matching and (b) phase matching with θ-variation or f-θ-variation techniques.

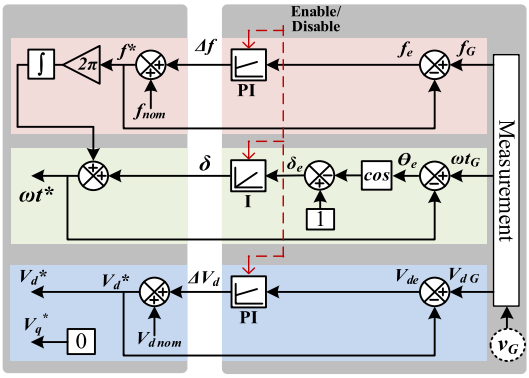

Fig. 5. Proposed presynchronization control.

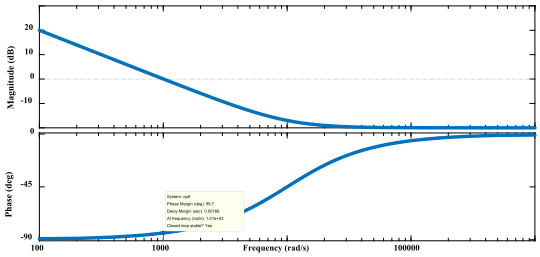

Fig. 6. Bode plot for OLTF of f-loop and V-loop.

among f-θ-V loops due to dependence on the measured signals from the microgrid for feedback control. In view of this, the present letter introduces a technique of presynchronization to provide swift and transient-free matching of f-θ-V through their exclusive loops, while avoiding the effects of these variables on each other. In addition, the proposed technique enables the master VSC to closely follow the AGFS output even if the latter varies during an ongoing synchronization process.

II. Proposed Presynchronization Technique

To connect the AGFS with the microgrid, the presynchronization control matches f-θ-V of the microgrid with those of the incoming AGFS by setting the reference commands for master VSC (see Fig. 1). For seamless connection of the AGFS, the proposed technique uses exclusive control loops to deal with f-θ-V of the microgrid (see Fig. 5), and it functions with the following unique features.

1) All control loops are enabled simultaneously. This provides fast sync, especially while dealing with a weak AGFS.

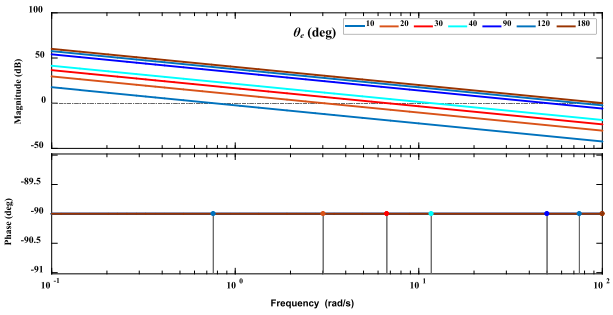

Fig. 7. Bode plots for OLTF of θ-loop for different values of θe.

2) The separate f-loop helps in f matching without influence of θ-error, thereby eliminating the f transients, which were observed in the earlier techniques. At the same time, the θ-loop reduces θ-error due to initial θ mismatch and any subsequent θ mismatch resulted from f control action. This reduces f-θ interplay to some extent.
3) The f-loop is designed for much faster response w.r.t. θ-loop. Such design allows quick f matching and maintaining the match even during the disturbances. Nearly locked f helps avoiding additional θ deviations, thereby eliminating θ transients and almost eliminating interplay of f-θ. Such design also helps to quickly set the disturbance signal $2\pi f^* t$ of the θ-loop so that the f-loop does not influence the θ-loop anymore due to frequency errors.
4) The phase-error signal is used in form of $(1 - \cos\theta_e)$ function. This eliminates the θ_e jumps at the input of the θ loop and the resulting θ jumps and V transients. This also ensures convergence to zero phase-error.
5) The θ-loop has only integral (I) controller. The absence of proportional (P) controller helps eliminating initial θ jump and the resulting V transient upon enabling the control.
6) Instead of using a measured quantity, the feedback signal in each control loop is obtained from the updated reference command of the respective loop. Since measured quantities of the microgrid are not used as feedback, the dynamics of the microgrid and measurement are not involved. This effectively makes the control design independent of plant and almost eliminates interaction among the f-θ-V loops, saves calculation efforts and improves the response speed of the control.

The f-loop processes error f_e between the measured AGFS frequency f_G and microgrid frequency f^* through a PI controller. It produces deviation Δf desired in the microgrid frequency, which is added with the nominal frequency f_{nom} to give updated f^* matching with f_G. The relations governing the f-loop at k^{th} sample are

$$f_e^k = f_G^k - f^{*k} \tag{1}$$

$$\Delta f^k = \Delta f^{k-1} + k_{pf}\left\{f_e^k - f_e^{k-1}\right\} + k_{if} f_e^k \tag{2}$$

$$\text{and } f^{*k} = f_{\text{nom}} + \Delta f^k. \tag{3}$$

The θ-loop takes the phase-error θ_e between the measured AGFS phase ωt_G and microgrid phase ωt^*, and processes

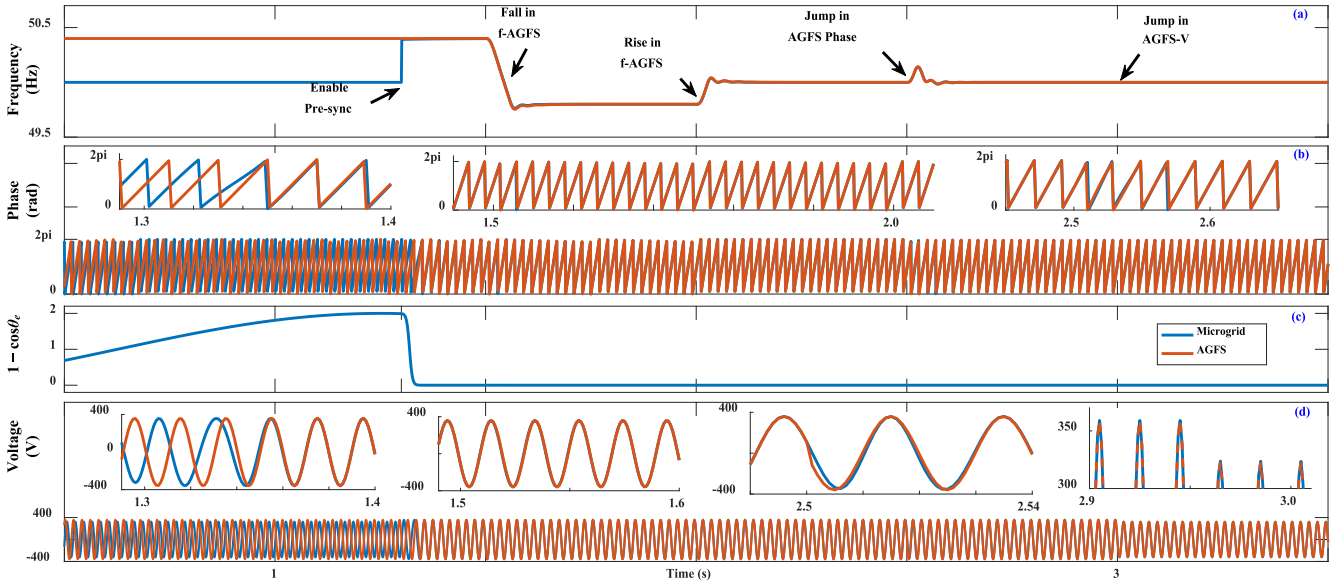

Fig. 8. Simulation performance during pre-synchronization: (a) frequency, (b) phase, (c) $(1-\cos\theta_e)$, and (d) voltages of microgrid and AGFS.

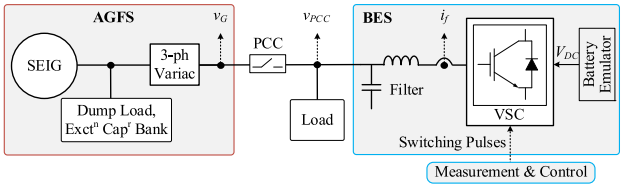

Fig. 9. Schematic diagram of experimental setup of microgrid.

"$1-\cos\theta_e$" via an integral (I) controller. It produces deviation δ desired in the microgrid phase, which is added with real-time phase $2\pi f^* t$ of the microgrid to give updated ωt^* matching with ωt_G. The relations governing θ-loop are

$$\delta_e^k = 1 - \cos\theta_e{}^k \tag{4}$$

$$\theta_e^k = \omega t_G^k - \omega t^{*k} \tag{5}$$

$$\text{and } \delta^k = \delta^{k-1} + k_{i\delta}\delta_e^k. \tag{6}$$

The V-loop processes the error V_{de} between the measured AGFS voltage V_{dG} and microgrid voltage $V_d{}^*$ through a PI controller. It produces deviation desired in the microgrid voltage ΔV_d, which is added with the nominal voltage $V_{d\ \text{nom}}$ to give updated $V_d{}^*$ matching with V_{dG}. The relations governing the V-loop are

$$V_{de}{}^k = V_{dG}{}^k - V_d^{*k} \tag{7}$$

$$\Delta V_d^k = \Delta V_d^{k-1} + k_{pv}\left\{V_{de}^k - V_{de}^{k-1}\right\} + k_{iv}V_{de}^k \tag{8}$$

$$\text{and } V_d^{*k} = V_{d\ \text{nom}} + \Delta V_d^k. \tag{9}$$

The PI controller gains of the frequency, phase, and voltage loops are denoted by k_p and k_i with additional subscripts f in (2), δ in (6), and v in (8), respectively.

A. Interaction Among the Control Loops

In all the existing methods of presynchronization, the feedback signals for the control loops are obtained from the measured quantities of microgrid. Therefore, the action of any one control loop affects the output of the respective loop, i.e., one of the reference commands; and corresponding quantity of the microgrid. Although for a momentary period, but a change in any one quantity of the microgrid subsequently affects the measured values of all the three quantities. Therefore, the action of any one loop influences the operation of all the loops at least during the transient operation. Since the proposed method uses the updated reference commands of the individual control loop as a feedback signal for the respective local loop, it helps in avoiding influence of one loop on the other. Except a marginal influence of the f-loop on θ-loop only during a brief period of initial f matching, there is no other interaction among all the control loops. Such influence is reduced substantially by designing the f-loop response much faster as compared with that of the θ-loop.

B. Controller Design Considerations

Since the f-θ-V loops do not interact with each other, the stability of individual loops is analyzed to check the stability of the entire control system. For this purpose, the open-loop transfer function (OLTF) of each loop is derived to obtain the respective Bode plot. The f-loop OLTF is obtained as $(k_{pf} + k_{if}/s)$, where $k_{pf} = 0.1$ and $k_{if} = 1000$ determine the loop characteristics. The OLTF gain margin (GM) and phase margin (PM) are ∞ and 95.7° in the Bode plot (see Fig. 6), indicating a stable f-loop. Similarly, the V-loop, having the same OLTF, controller gains, GM and PM, is also stable.

Since the influence of f-loop on θ-loop is marginal due to 10 times faster response of f-loop, it is assumed that the frequency is already matched, the disturbance signal $2\pi f^* t$ has already settled, and the phase error is not influenced due to frequency

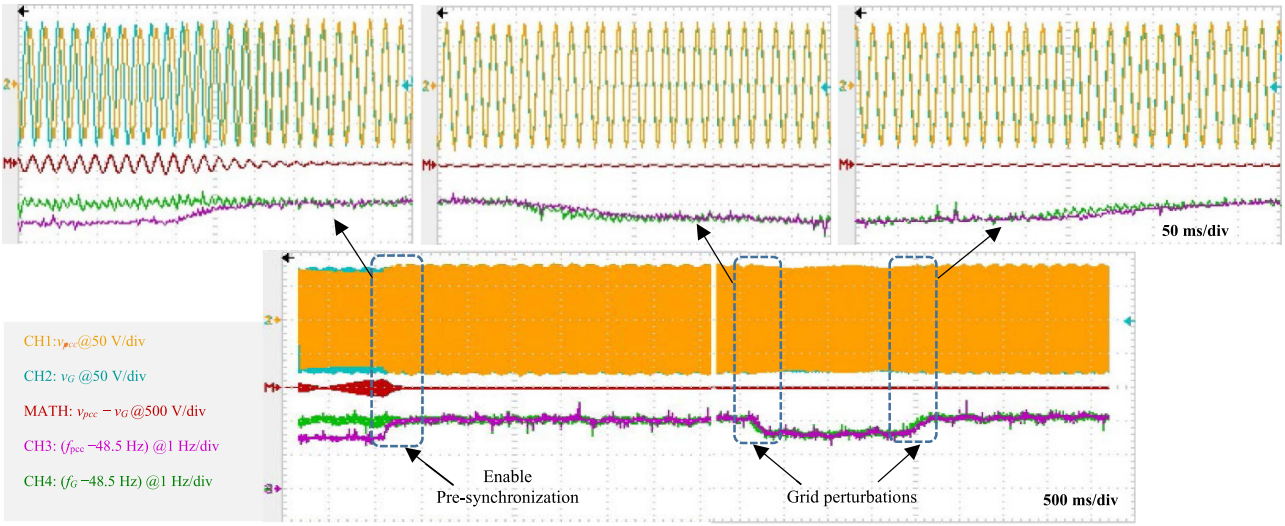

Fig. 10. Experimental performance of voltage, frequency and phase of microgrid and AGFS, and their voltage difference during: enable presynchronization, AGFS perturbations, and zoomed views of three encircled event.

error anymore. Thus, the θ-loop will compensate for the phase-error θ_e, which is independent of f-loop. Now, θ_e will reduce almost linearly under the influence of the integral controller of the θ-loop. Therefore, the OLTF of the θ-loop is obtained as $[(k_{i\delta}/s)\,(1 - cos\theta_e)]$, where $k_{i\delta} = 50$ along with θ_e determine the loop characteristics [14]. The GM and PM are ∞ and 90° for entire range of $-180° < \theta_e < 180°$ (see Fig. 7), indicating a stable θ-loop.

The closed-loop transfer function $T_f(s)$ of the f-loop (and similar one for V-loop) can be obtained as

$$T_f(s) = \left(1 + \frac{k_{pf}}{k_{if}}s\right) \Big/ \left(1 + \frac{1 + k_{pf}}{k_{if}}s\right) \tag{10}$$

which being a first-order system, and the choice of $k_{pf} << k_{if}$ for locating the pole far from the origin in the LHS of s-plane for ensuring stability [15], leads to the time constant T and settling time t_s of the f-loop as

$$T \approx \frac{1}{k_{if}} \text{ for } k_{pf} \ll k_{if} \text{ and} \tag{11}$$

$$t_s = 4T. \tag{12}$$

Similar expressions can be obtained for the θ-loop using its OLTF. To attain synchronization time frame of 40 ms, the settling time of the f-loop and V-loop is set as 4 ms, and that of the θ-loop is set as 40 ms. For these choices, the f-loop and V-loop PI gains are obtained as (0.1; 1000), and the θ-loop I gain is obtained as 50 for maximum phase error θ_e of $\pm 180°$.

III. Simulation Results

The model of the master-slave ac microgrid shown in Fig. 1 is developed in MATLAB/Simulink to test the performance of the proposed secondary control for presynchronization during various operating conditions. For the simulation study, the GF-VSC of the microgrid is operated at nominal voltage and frequency of 400 V, 50 Hz; and the AGFS is operated in the range of $\pm 10\%$ of the nominal voltage and $\pm 5\%$ of the nominal frequency.

Fig. 8 shows the simulation performance of the microgrid presynchronization with the incoming AGFS based on the proposed technique. The f-θ-V of both the sources are plotted. In addition, $(1 - \cos\theta_e)$ signal is also plotted. To demonstrate the capability of the proposed technique, after enabling the control, various perturbations are applied in the AGFS in terms of f-variations, θ-jump, and V-jump.

Initially the microgrid is operated at nominal V-f, and the AGFS is operated at 440 V and 50.4 Hz. At 1.3 s, the three loops are enabled simultaneously to start the presynchronization process. It is worth noting that $\theta_e = 180°$ at the instant of enabling the loops, which is a worst-case scenario. Even under such initial condition, the proposed technique takes about 2–3 cycles to match f-θ without notable jump or transient in both the quantities. The AGFS frequency is then reduced to 49.8 Hz at 1.5 s and subsequently it is raised to 50 Hz at 2.0 s, and the microgrid frequency closely follows these variations without affecting the presynchronization.

A θ-jump of 20° at 2.5 s is introduced in AGFS. It can be observed that the microgrid f-θ closely follow those of the AGFS. The proposed technique does this without introducing any θ-jumps in microgrid due to integral action of θ-control loop. At 3.0 s, a V-jump of -44 V, i.e., 10% of V-nominal, is introduced in AGFS, and once again the microgrid voltage is observed to be closely following the AGFS voltage. When a θ-jump occurs in the AGFS, a deviation of $\sim$0.1 Hz is observed in the measured frequency of one source and the other still continues to follow it quickly and closely. During the f or V disturbance, the matching is quickly attained without reflecting any deviation in the other quantities.

IV. Experimental Results

Fig. 9 gives schematic diagram of a laboratory test-bench built to validate the system performance. A weak AGFS is emulated using a controlled dc motor powered 3-Φ 0.75 kW SEIG followed by a variac, and it can be connected to the

microgrid via a switch. A bidirectional BES is built using a 5 kVA VSC with its dc side connected to a battery emulator and ac side connected to the microgrid PCC via an *LC* filter. The control algorithm is implemented on TI MCU TMS320F28335 via code composer studio.

The BES VSC is operated with closed-loop GF control to supply scaled down voltage of 50 V, 50 Hz at the PCC. Initially, the AGFS provides ∼55 V, ∼50.5 Hz. On enabling the pre-synchronization loops, the *f*-θ-*V* of PCC are matched with AGFS output in ∼5 cycles without any noticeable transient, as seen in the first zoomed view in Fig. 10. The other two zoomed views show a fall and a rise in the AGFS frequency. The AGFS voltage also falls and rises along with frequency. These variations in the AGFS *f*-*V* are followed by the PCC *f*-*V* quite swiftly in ∼1 cycle range. This shows that any disturbance in the AGFS even during the presynchronization does not delay the process.

V. Conclusion

It is important to maintain transient-free operation of microgrid during the presynchronization, since the phase and frequency disturbance affect the performance of the connected loads as well as the other grid-following VSCs [16]. This is ensured by the proposed presynchronization technique, which sets the commands for the primary control using exclusive loops for matching the frequency, phase, and voltage magnitude, each. The fast frequency loop enforces a quick frequency match without influence of the phase-error, while the integral-controller-based phase loop negates the phase-error without causing phase jumps. This improves the presynchronization speed by avoiding phase-frequency interplay, and makes this technique effective while dealing with a weak grid. The use of feedback control signals obtained from the updated reference commands saves the calculation efforts and further improves the response speed. In aaddition, this method of using local feedback allows the controller to avoid the plant and measurement dynamics, and thereby almost eliminating the interaction among the control loops. The results show transient-free matching of the variables in ∼5 cycles and any change in the AGFS output being closely followed by the grid-forming converter, thereby enabling swift presynchronization.

References

[1] J. Hu, Y. Shan, K. W. Cheng, and S. Islam, "Overview of power converter control in microgrids—Challenges, advances, and future trends," *IEEE Trans. Power Electron.*, vol. 37, no. 8, pp. 9907–9922, Aug. 2022.

[2] *IEEE Standard for Interconnection and Interoperability of Distributed Energy Resources With Associated Electric Power Systems Interfaces*, IEEE Standard 1547-2018, Revision of IEEE Standard 1547-2003, 2018, pp. 1–138.

[3] K.-H. Tan and T.-Y. Tseng, "Seamless switching and grid reconnection of microgrid using petri recurrent wavelet fuzzy neural network," *IEEE Trans. Power Electron.*, vol. 36, no. 10, pp. 11847–11861, Oct. 2021.

[4] A. Banerjee et al., "Autonomous restoration of networked microgrids using communication-free smart sensing and protection units," *IEEE Trans. Sustain. Energy*, vol. 14, no. 2, pp. 1076–1087, Apr. 2023.

[5] J. Chen, S. Hou, and J. Chen, "Seamless mode transfer control for master–slave microgrid," *IET Power Electron.*, vol. 12, pp. 3158–3165, 2019.

[6] B. Singh, G. Pathak, and B. K. Panigrahi, "Seamless transfer of renewable-based microgrid between utility grid and diesel generator," *IEEE Trans. Power Electron.*, vol. 33, no.no. 10, pp. 8427–8437, Oct. 2018.

[7] S. Shah, H. Sun, D. Nikovski, and J. Zhang, "VSC-based active synchronizer for generators," *IEEE Trans. Energy Convers.*, vol. 33, no. 1, pp. 116–125, Mar. 2018.

[8] K. Shi, W. Song, H. Ge, P. Xu, Y. Yang, and F. Blaabjerg, "Transient analysis of microgrids with parallel synchronous generators and virtual synchronous generators," *IEEE Trans. Energy Convers.*, vol. 35, no. 1, pp. 95–105, Mar. 2020.

[9] M. Chankaya, A. Ahmad, I. Hussain, B. Singh, and S. B. Q. Naqvi, "Grid-interfaced photovoltaic–battery energy storage system with slime mold optimized adaptive seamless control," *IEEE Trans. Ind. Appl.*, vol. 58, no. 6, pp. 7728–7738, Nov./Dec. 2022.

[10] C. Wang, B. Liang, and J. He, "An enhanced power regulation and seamless operation mode transfer control through cooperative dual-interfacing converters," *IEEE Trans. Smart Grid*, vol. 9, no. 6, pp. 5576–5587, Nov. 2018.

[11] V. Jain, S. Kewat, and B. Singh, "Three phase grid connected PV based EV charging station with capability of compensation of reactive power," *IEEE Trans. Ind. Appl.*, vol. 59, no. 1, pp. 367–376, Jan./Feb. 2023.

[12] P. J. Chauhan, B. D. Reddy, S. Bhandari, and S. K. Panda, "Battery energy storage for seamless transitions of wind generator in standalone microgrid," *IEEE Trans. Ind. Appl.*, vol. 55, no. 1, pp. 69–77, Jan./Feb. 2019.

[13] C. N. Papadimitriou, V. A. Kleftakis, and N. D. Hatziargyriou, "Control strategy for seamless transition from islanded to interconnected operation mode of microgrids," *J. Mod. Power Syst. Clean Energy*, vol. 5, no. 2, pp. 169–176, Mar. 2017.

[14] M. Amin and Q.-C. Zhong, "Resynchronization of distributed generation based on the universal droop controller for seamless transfer between operation modes," *IEEE Trans. Ind. Electron.*, vol. 67, no. 9, pp. 7574–7582, Sep. 2020.

[15] A. O'Dwyer, "PI and PID controller tuning rules: An overview and personal perspective," in *Proc. IET Ir. Signals Syst. Conf.*, 2006, pp. 161–166.

[16] A. Ahmad, H. D. Tafti, G. Konstantinou, B. Hredzak, and J. E. Fletcher, "Distributed photovoltaic inverters' response to voltage phase-angle jump," *IEEE J. Photovolt.*, vol. 12, no. 1, pp. 429–436, Jan. 2022.